

Development of a New Controller for Solar Home System: PWM Charge Controller & DC to DC Converter (12V to 120V)

Mohammad Shariful Islam, Hasmaini Mohamad* and S.Z. Mohammad Noor

Abstract— Solar Home System (SHS) is a stand-alone power solution in isolated places where there is no connectivity to the national power grid. Currently, an off-grid SHS has a solar panel, a lead-acid battery, a Pulse Width Modulation (PWM) solar charge controller, and 12V DC power operated electrical home appliances; in some cases, a DC to DC converter or a DC to AC inverter has been connected. So far, various SHS packages have been introduced, each with a set of product features and prices. Since the majority of SHS are small in size, producing energy is inadequate to satisfy the customer's demand. This study introduces a new feature that incorporates both analog PWM solar charging techniques and a DC to DC (12V to 120V) converter to satisfy the needs of existing off-grid SHS users. The design of solar charging includes improved charging techniques i.e surge voltage and lightning protection. The result produced is a noise-free switching gate drive signal and high-performance fixed-frequency current mode controllers. The new controller's design also reduces the number of devices in the SHS; thus reduces the controller's total production cost.

Keywords: Pulse Width Modulation, fixed frequency current mode, noise free gate drive signal, charging efficiency, self-power consumption, reduce the number devices.

I. INTRODUCTION

SOLAR energy alone has seen significant growth in recent years. Photovoltaic (PV) innovation is the most promising, advantageous, and promising of all green technologies for converting solar energy into electrical energy, with or without battery backup. Primarily in third-world countries, it appears that there is a lack of electrical energy, which has influenced rural areas. However, the World Bank and the International Development Agency have launched an off-grid solar home

system in that area to facilitate the community in carrying out their daily tasks such as cooking, working, and studying [2]. People in rural areas have significantly changed their lifestyles in order to incorporate a stand-alone solar home system (SHS).

The manufacturer initially introduced the solar home system in a variety of products and services with varying sizes of solar modules including 30Wp, 40Wp, 50Wp, 65Wp, 80Wp, 100Wp, and 120Wp [14]. SHS components include a solar panel, a lead-acid battery, a charge controlling device, and a suitable load predicated on the needs of the customer. The features of the charge controlling devices and various DC powered loads have indeed been developed. The three generations of the SHS have been segmented according to the upgrading of the solar home system of components. Whenever the solar home system solution was first launched, it included some components such as a solar panel, lead-acid battery, solar charger, 12V powered DC lamp, black and white television, radio, and so on. The load was connected at a limited distance, where all components connected to flow high current through the cables. Initially, when the solar charge controller was used as a voltage regulator device, the charging efficiency was not maintained. In [13] solar charging systems and 12V DC powered loads were upgraded, and a new feature enhancement system was launched by Infrastructure Development Company Limited (IDCOL); that features are PWM solar charging mechanism, mobile phone and LED lantern charging port.

In [1], charge controller functions were designed on the principle with PWM controlled DC to DC converter for charging the battery. The PIC microcontroller was used to implement PWM charging techniques, but certain crucial considerations were not established such as self consumption, electromagnetic interference (EMI) surge voltage and lightning safety. In [7] & [15], charging controls are used mostly based on the Single-ended primary-inductor converter (SEPIC) PWM technique. The SEPIC-based converter is often used in battery-powered operating devices. A PWM-based charge controller can be used to maximize output power depending on the temperature of both panel and irradiance conditions. In [8] and [25], the solar charge controller was designed to monitor the charging level of the maximum power point. This power of

This manuscript is submitted on 20th October 2021 and accepted on 26th January 2022.

Mohammad Shariful Islam, Hasmaini Mohamad and, S.Z. Mohammad Noor are with the School of Electrical Engineering, College of Engineering, Universiti Teknologi MARA, 40450 Shah Alam, Selangor (e-mail: hasmaini@uitm.edu.my)

*Corresponding author
Email address: hasmaini@uitm.edu.my

1985-5389/© 2022 The Authors. Published by UiTM Press. This is an open access article under the CC BY-NC-ND license (<http://creativecommons.org/licenses/by-nc-nd/4.0/>).

solar panel was transferred to the battery for effective performance comparison which includes Perturb and Observes (P&O) method. It is not a suitable controller for the small size of applications and it is suitable for large scale solar systems. In [11] and [30], the basic system includes discrete time control as well as PI-compensator were used to track the maximum power points (MPPs) of the solar panel. The framework has been held tight to the Maximum Power Point Tracker (MPPT), consequently achieving the maximum allowable transfer of power from the solar array. Nevertheless, this design was suitable for more than 1kW solar system. If those are key design parameter, it must be considered in the design or probably lightning protection, self consumption and etc is just additional factors that can be considered to improve the system performance.

In [2], the system has difficulty to accurately configure and optimize the solar charging mechanism. It is ideal for a large-scale solar home device under shielded grid-connected areas; where the input voltage was 48V DC and used the Li-Ion battery. In [22], the PV input voltage was fed to both the dc-dc converter as well as to the single-phase inverter. In [13], this design was performed through a DC-DC converter or Buck converter that employs a programmable micro-controller to convert energy using a DC-AC inverter into a widely accessible form. Remote users could use a 12V DC solar home system, however there are some limitations at the customer's end. The self-consumption of solar charger is enormous. The primary way for most solar homes and businesses to save energy is to reduce self-consumption as it is connected to the system for 24 hours. In [35], [36], [37], and [38], Switch Mode Power Supplies (SMPS) were created to rapidly change voltage and current because of DC-DC power converters. This enables surrounding devices and input power lines to be interrupted by EMI noises. Consequently, EMI noises become a major issue.

In [3], control criteria, energy storage management, and the DC-AC inverter or DC-DC converter are all necessary aspects of an off-grid solar home system. A controller device oversees the charging and discharging of the energy storage mechanism. A DC-AC function is to convert energy into a form which can be used instantly. This device is important, because of preponderance of equipment operate using AC power.

Currently, power electronics engineering has smartly introduced the most reliable power solution. An incandescent light bulb would shine equally brightly when powered by 120V DC or 120V RMS AC. DC high voltage PWM IC would run from 80V to 450V DC voltage. So, laptop, fan, LED TV and standard AC products can run on high voltage DC (120V), and the power conversion loss will minimize. Other hand, DC to DC conversion (12V to 120V) is a procedure for minimizing power loss to transmit power at the desired load end. Due to high voltage DC means that the total energy is passed in smoothly as per load required which cause voltage values will be high and the current values will be low so that the power will be transmitted with the full load requirement to minimize power loss. Minimizing power loss is a key factor in the SHS. Also, due to limited wires, there has a barrier to connecting the load.

However, the power conversion unit and the charge controller are separate devices, while the two devices have separate self-consumption, although the power conversion loss is more than 30%. In special cases, it is difficult to convert the power from 12V DC to 220V AC with minimum power loss. Therefore, conversion unit and PWM solar charger is compacted as a design of new controller for existing off-grid solar system.

Therefore, it is important to consider minimizing self power consumption, surge protection, minimizing product's cost in the controller design. The contribution of this research project are as follows:

1) To develop a new analog PWM converter that used a fixed frequency current controlling algorithm to reduce EMI noise in an off-grid solar system.

2) To design a compact single-stage boost DC to DC flyback converter integrated with the designed analog PWM charge controller for the existing off-grid solar system. It will reduce the number of devices to maintain the noise-free switching gate signal.

3) To reduce the designed controller's self-power consumption. As it has been connected for 24 hours, it is critical to reduce the system-connected controller's self-power consumption.

In this study, PWM solar charging circuit and DC-DC (12V - 120V) converter are designed using Altium, LT-spice, PI Expert and Proteus. Two functional circuits are combined in a single circuit using same reference parameters considering decrement of self-power consumption. In the proposed research work, compact design of the main circuit integrated with the controller are created with certain element and criteria for reliability of the system.

II. RESEARCH FRAMEWORK

It is important to consider the optimization parameters of solar charging circuits. There have been issues in developing some design topologies for PWM solar charger and DC-DC converter.

PWM is a technique for tracking an analog signal and producing a digital output. By comparing the ramp or carrier signal with the error between the desired output voltage signal and the true output voltage signal, the PWM constant frequency signal can be obtained.

Three major topological components dominate the output of the fly-back converter: the primary switch, the secondary rectifier, and the transformer. The transformer has a significant impact on converter efficiency as a single feature. Buck-boost and flyback converters are effectively lossless resistors when operating under interrupted conditions. The open loop of these converters controls the waveform.

The Fixed Frequency Current Mode algorithm has evolved into a dynamic self-supply mechanism that significantly simplifies the configuration of the auxiliary supply and voltage common collector (Vcc) capacitor by enabling internal startups, transients, latch standby, and other features. Dynamic self-

supply is important for keeping the controller alive when no switching pulses are accessible, including when the controller is blown out, or to keep the controller from stopping during a transient load when Vcc can drop. It also contains a timer-based

fault detection mechanism for overload detection and dynamic compensation to ensure maximum power despite of input voltage. Fig.1. show the block diagram of the research framework-

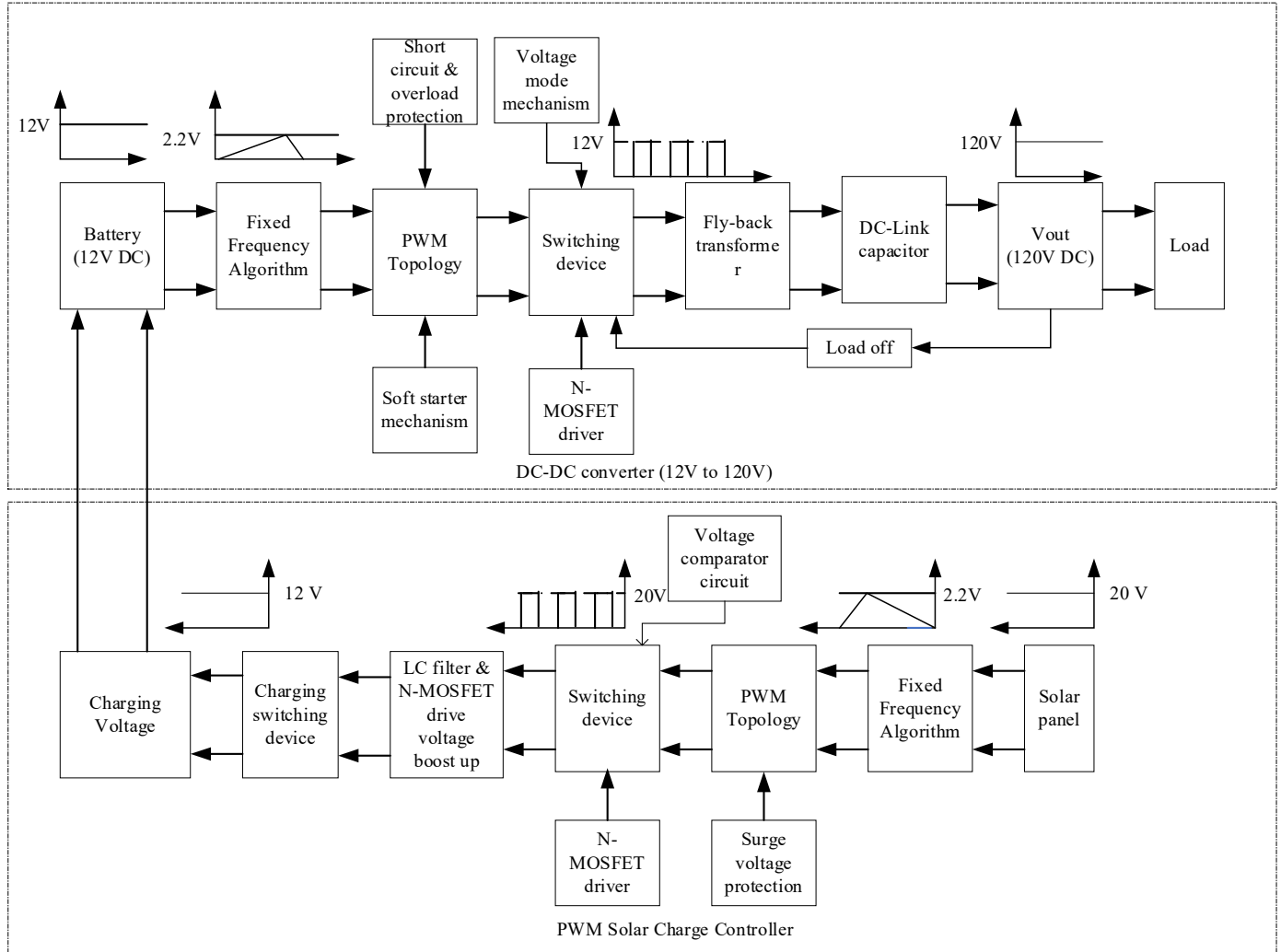


Fig.1. Overall block diagram of research framework.

III. DEVELOPMENT OF A NEW CONTROLLER

The new controller for solar charging circuit based on fixed frequency current mode controller is simulated using LT-Spice software. Detail design of each controller’s component is explained in this section.

A. Designing the fly-back transformer

A specific method for selecting the inductance value is defined, and the inductance value and turn of ration are calculated based on the transfer power and switching frequency. The two inductance values are set up parallel in the primary side with respect to the secondary inductance due to flow the high current at primary end. The energy that accumulates in the magnetic field is transmitted to the output capacitor as well as the load during the fly-back operation.

B. Designing the gate drive circuit

In semiconductor devices, gate drive circuits can be used to improve the performance. The N-MOSFET gate drive circuit limits or stops the amplitude and rate of rise of the switching voltage, reducing power consumption. The simplest drive circuit consists of a resistor and a capacitor connected by a thyristor or transistor. NPN and PNP transistors can be used to create the circuit, which is the path for discharging the gate capacitance of an N-channel MOSFET. Fig.2. show the block diagram of gate driver circuit –

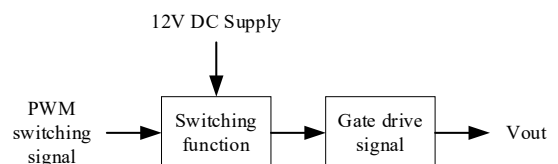


Fig.2. Block diagram of gate driver

C. Soft start

PWM signal initiates at zero duty cycle but has no internal soft-start control. Thus soft start mechanism as shown Fig.3 is designed using the combination of PNP transistor, resistor, and capacitor.

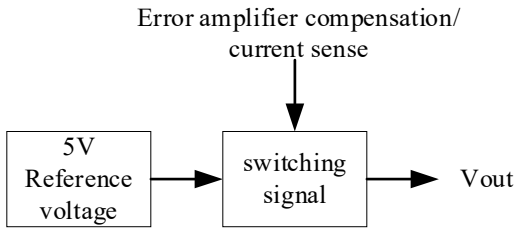


Fig.3. Block diagram of soft start mechanism

D. Voltage mode

The transformer's primary winding current is converted to voltage based on the transformer's secondary winding turn ratio. Fig.4 shows the voltage mode mechanism adopted in this study. A saw-tooth waveform acts as an input signal to be used at the current sense terminal through an oscillating timing capacitor & resistor, and then that signal is compared to the error voltage. The error amplifier is compared to the artificial ramp voltage using a PWM comparator.

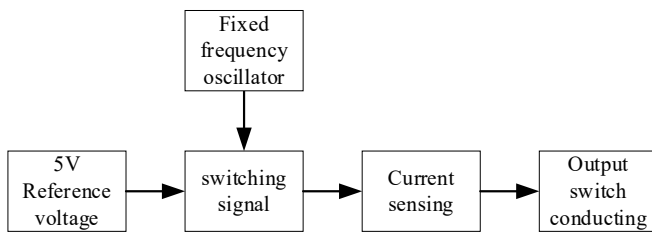


Fig.4. Block diagram of voltage mode mechanism

E. Designing the N-MOS gate drive

The charge on the boot condenser must applied in maintaining the high-side transition for N-MOSFET. Because of drain to source voltage is just lower than gate to source voltage. Fig.5. is used to N-MOSFET gate driver mechanism.

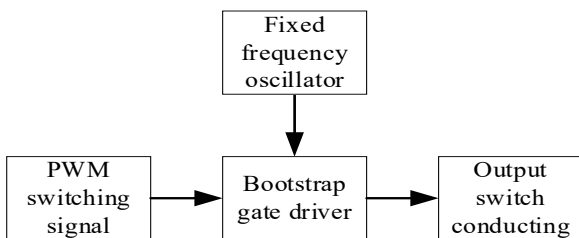


Fig.5. Block diagram of N-MOSFET driver for solar charger

F. Techniques for reducing the self-power consumption

There have been two techniques implemented to minimize self-power consumption: The following are specific elements of the technique-

i. The dedicated off program enables the fixed-frequency current control mode to accomplish exceptionally low no-load input power consumption through "sleeping" the entire system.

Based on frequency fold-back, the controller has exceptional efficiency in light load conditions even as consuming very small stationary power. Specific frequency, ramp compensation, and versatile latch feedback enable the controller to generate an excellent output for the desired design.

ii. The controller utilizes an LCD and LED display as system status indicators: this system status should be publicized two to three times each day, for just roughly 30 seconds. However, that power is employed for 24 hours, it is also one type of power consumption. This function is served by the push switch circuit mechanism, which is comprised of an Op-amp and an NPN transistor- as shown in Fig.6.

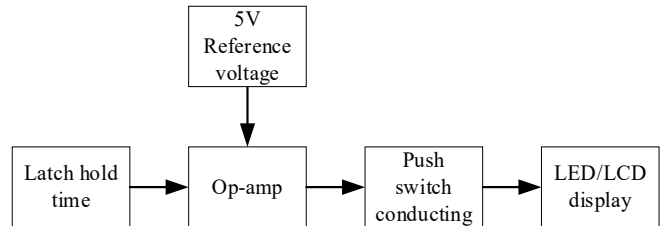


Fig.6. Block diagram of push switch technique

G. Designing the voltage comparators

Fig.7. shows the block diagram of voltage comparator. The two input voltages are compared by a voltage comparator. The Op-amp voltage comparator is used as a simple circuit that demonstrates the threshold stress and hysteresis width.

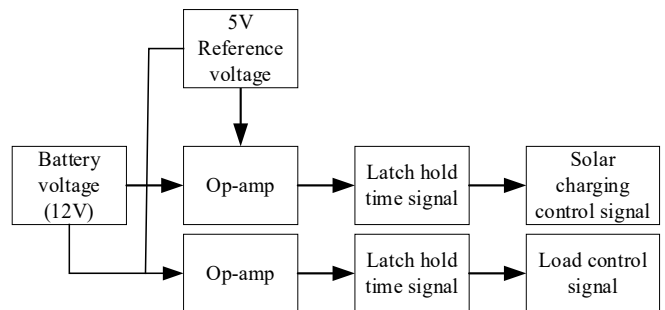


Fig.7. Block diagram of voltage comparator

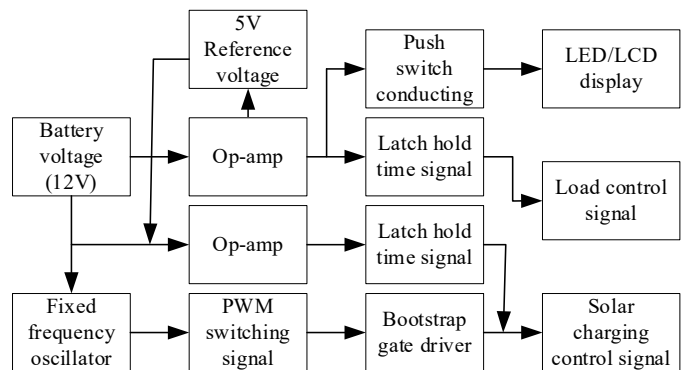


Fig.8. Block diagram of solar charger

The operational amplifier determines the various voltage switching thresholds depending on the battery's voltage conditions. These have two major switching components: one is for solar charging with a battery and the other for a load

connected to a battery. The hysteresis potential difference between both the solar charging disconnect and reconnected points is 0.7V. The hysteresis voltage difference between the load disconnect and reconnect statements seems to be 1V. The PNP transistor and resistor voltage dividing programming are being used to set the hysteresis threshold values.

IV. RESULTS AND DISCUSSION

Analog PWM comparator with eight characteristics including current limit control or sinks peak current, feedback voltage loop for stability, slope compensation, oscillation timing for fixed-frequency operation, signal and power returning ground, PWM drive waveform signal for N-MOSFET can be seen in Fig:9, Vcc clamp voltage source, and voltage reference for the timing resistor (RT) and timing capacitor (CT) were used to fix the oscillation timing; where the RT resistor is connected to the reference voltage and the CT capacitor is connected to ground. The fixed frequency oscillation timing (focs) has been delineated by the RT/CT values, using the formula in Equation (1).

$$f_{ocs} = \frac{1.72}{R_{RT} \times C_{CT}} = \frac{1.72}{12K \times 220P} = 651.5 \text{ kHz} \dots (1)$$

The waveform for the fixed frequency algorithm is seen in the Fig 9 and 10. Timing resistor values should be greater than 5K and timing capacitor values should be between 1nF and 100nF. The total supply current tends to vary with the output current, as well as the quiescent current is 0.5mA. The function has been either continuous conducting method (CCM) or discontinuous conducting method (DCM). It depends on the input voltage and loading condition (DCM) at the output terminal. PWM controller output can be shut down to sink current or command zero duty cycle by applying an external voltage to the PWM controller's compensation. For system stability, the feedback voltage (V_{FB}) should be less than 1.5V. This voltage is obtained from the error amplifier's inverting input. The current sense (I_{SENSE}) terminal is connected between the source of the MOSFET and the sense resistor to add the slope compensation of a voltage ramp, where R_{SENSE}, resistor value is less than 0.05, V_{SENSE} voltage is 1 volt, that peak I_{SENSE} defines the following formula –

$$I_{SENSE} = \frac{V_{SENSE}}{R_{SENSE}} = \frac{1}{0.05} = 20A \dots (2)$$

According to Equation (2), short circuit protection current and overload protection current are decided by the value of R_{SENSE} resistor and its across the voltage. The I_{SENSE}, signal is a noninverting signal that is compared to that same error gain voltage to make sure the device's reliable operation. The effect of even a high impedance supply rail in comparison to the ground is an issue when it comes to noise-free PWM signal. Because of snubber circuit is used at the PWM driver's output terminal, one PNP transistor and one NPN transistor are used to ensure a noise-free N-MOSFET drive gate PWM signal. MOVs (Metal Oxide Varistor) have been connected in series to the solar panel port to prevent surge voltage triggered by lightning.

The voltage of a sawtooth wave is determined by the value of the timing resistor (RT) and the value of the timing capacitor

(CT). The red waveform represents a sawtooth wave, and the green waveform represents the PWM switching signal that follows the sawtooth wave. Because of the high impedance supply rail in regards to ground, this same noise-free gate drive signal is completely reliant on V_{CC} voltage, which is combined with V_{IN} capacitor (C7= 2200F). Fig 8 illustrates the block diagram of the solar charging portion.

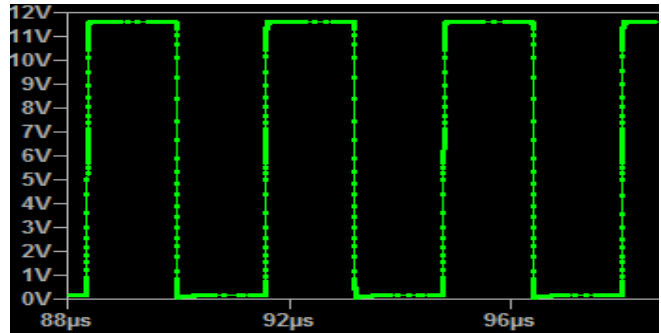


Fig.9 PWM drive signal for N-MOSFET

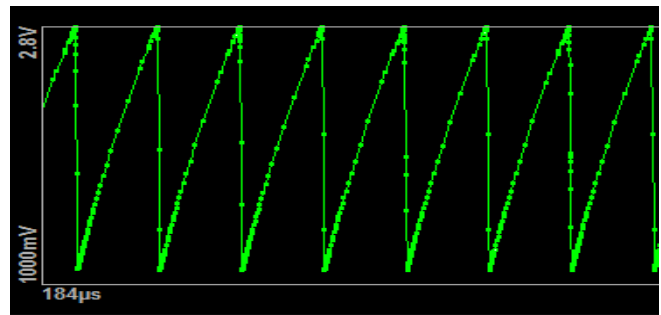


Fig.10. Waveform of voltage ramp.

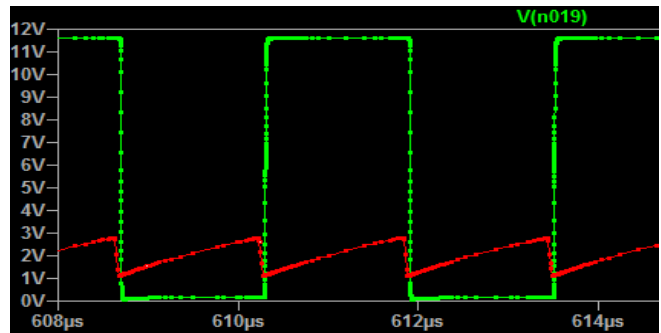


Fig.11. Waveform of voltage ramp and PWM output

Table.1. show the switching alignment according to the various conditions of battery voltage. Proposed PWM charge controller integrated with DC to DC converter: The DC-DC offline converter is designed using fixed frequency current mode algorithm, that is implemented by certain peripheral components. Current limit control or peak current sinking, feedback voltage loop for stability, slope compensation, oscillation timing for fixed-frequency operation, signal & power returning ground, PWM drive signal for N-MOSFET, Vcc Clamp voltage source, and voltage reference for error amplifier all are features of this analog PWM comparator. The fixed frequency value is defined by the timing resistor and

capacitor. A timing resistor (R3=12K) connects Vref and RT/CT, and a timing capacitor integrates RT/CT and GND: Therefore, the frequency of oscillation can be defined by the equation 3 –

$$f_{sw} = \frac{1.72}{R_{RT} \times C_{CT}} = \frac{1.72}{12K \times 330P} = 434 \text{ KHz} \dots\dots\dots(3)$$

TABLE I
SWITCHING ALIGNMENT ACCORDING TO THE VARIOUS CONDITIONS OF BATTERY VOLTAGE

No of case	Battery voltage	Load condition	Switching status	Functional status
Case no - 1	14.5V	10A	High Voltage Disconnect (HVD)	<ul style="list-style-type: none"> Solar charging is disconnected Load connected Battery full charged
Case no - 2	13.8V	10A	High Voltage Reconnect (HVR)	<ul style="list-style-type: none"> Solar charging is reconnected Load connected Battery status is healthy
Case no- 3	11.5V	10A	Low Voltage Disconnect (LVD)	<ul style="list-style-type: none"> Solar charging is connected Load disconnected Battery status is deep discharged
Case no- 4	12.5V	No-load	Low Voltage Reconnect (LVR)	<ul style="list-style-type: none"> Solar charging is connected Load reconnected Battery status is fit for discharge

The output switching frequency (f_{sw}) is determined by the frequency of oscillation (f_{osc}). The timing resistor should be assigned a rating greater than 5K.

It has distinctive advantages, such as the potential to generate the switching pulse in undervoltage lockout mode with a startup current of less than 1mA. Throughout a transistor-based snubber circuit, a PWM switching signal drives the gate of an N-channel MOSFET. The cause of 434 kHz oscillation signals has induced capacitance at the gate of N-Channel MOSFET, having caused the original PWM signal to be destroyed with respect to equation (3). A snubber circuit will ensure the gate signal is noise-free. For overshoot and undershoot voltage protection, a Schottky diode (MUR460) is connected at the gate of an N-MOSFET (IRFP250N). It has a high impedance from the supply rail to ground, and the input and output share the common ground point. V_{CC} power line is the main supply of output current, which can be controlled by a current limiting resistor (R9= 1000K). This circuit's quiescent current is 0.5mA. The total output current depending on the gate charge of external power N-MOSFET (Q_g) and switching frequency (f_{sw}). Switching frequency (f_{sw}) is equal to oscillation frequency (f_{osc}). The output drive current can be calculated using the following formula-

$$I_{OUTPUT} = Q_g \times f_{osc} = Q_g \times f_{sw} [f_{osc} = f_{sw}] \dots\dots\dots(4)$$

MOSFET gate drive resistor (R6= 10Ω) is power resistor, switching loss minimization and EMI performance depends on

this resistor. PWM comparator has a noninverting current sense port, that can be compared proportionally between the voltage across R_{SENSE} and the voltage of error amplifier output. Typically, V_{SENSE} voltage is 1V, where it has a RC filter (C10: 100nf and R5: 1KΩ) for balancing the capacitive load. The time constant of the RC filter is less than oscillation timing. The PWM comparator has a compensation port, that can be performed two acts with 1MHz bandwidth, which are the source and current sink. This port can be grounded by an NPN transistor to shut down the system in external force. Pulse width modulation signal starts at zero duty cycle, so it needs to add a soft start mechanism at the compensation point. It is designed using three components, are resistor (R19: 100Ω), capacitor (C13: 10nf), and PNP transistor (Q4). V_{REF} is a 5V voltage source bypass the ground, which provided charging voltage for oscillation timing and act as an independent voltage source.

The selected transformer is designed to double winding turn at primary side cause of low voltage high current path, while the secondary winding has single turn cause of high voltage low current path to consider the switching frequency of 434 kHz. Magnetizing inductance depends on the continuous conducting mode of the duty cycle. The primary side of the transformer is connected with a drain of N-MOSFET (IRFP250N) and a single-phase ultrafast power diode (D5: MUR460). It is connected with a parallel RC filter (R10: 220KΩ & C7: 13.8nf) cause of protecting the primary winding at the off condition of the duty cycle. The maximum turn ratio of the transformer depends on the reflected voltage (V_{REF}) and output voltage (V_{OUTPUT}). Primary to secondary turn ratio is calculated using the following formula:

$$N_{PS} = \frac{V_{REFLECTED}}{V_{OUTPUT}} \dots\dots\dots(5)$$

Desired voltage rating of N-MOSFET and output voltage rating depend on the primary to secondary turn ratio of the transformer. Fig.12. shows the desired block diagram of DC-DC converter –

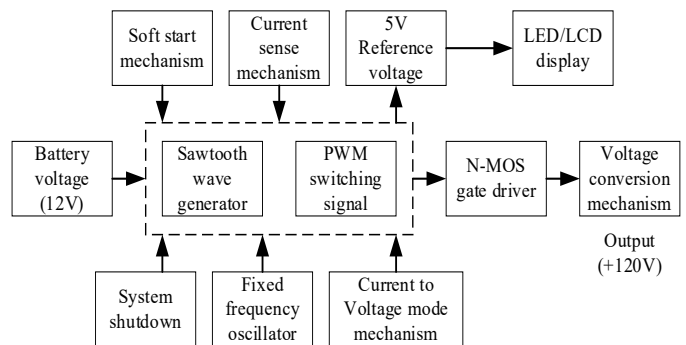


Fig.12. Block diagram of DC-DC converter

The level of conversion voltage is determined by the transformer's secondary turn ratio, N-MOSFET, ultrafast power diode, and output capacitor. The capacity of power conversion is based on the properties of the core, winding wire, and core size. It is a straightforward procedure for converting DC voltage to use the fixed frequency current control mode algorithm to

obtain DC 120V from a DC 12V supply.

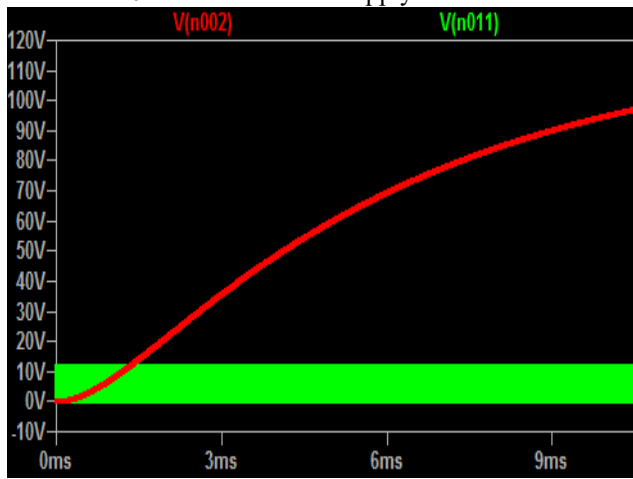


Fig.13. Voltage waveform of Input & output (Vn002 – Red color: Output voltage waveform & Vn011 – green color: MOSFET- gate drive voltage waveform)

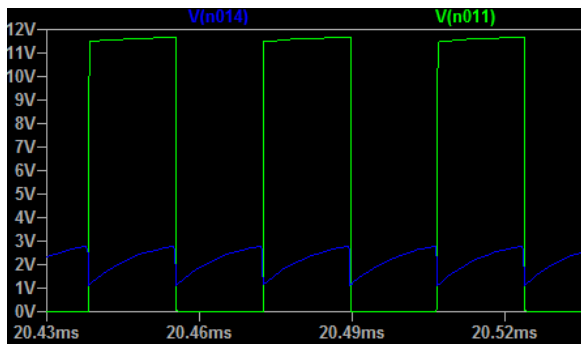


Fig.14. Waveform of MOSFET gate drive & oscillation timing (Vn011 – green color: MOSFET gate drive switching waveform & Vn014 – blue color: oscillation timing waveform).

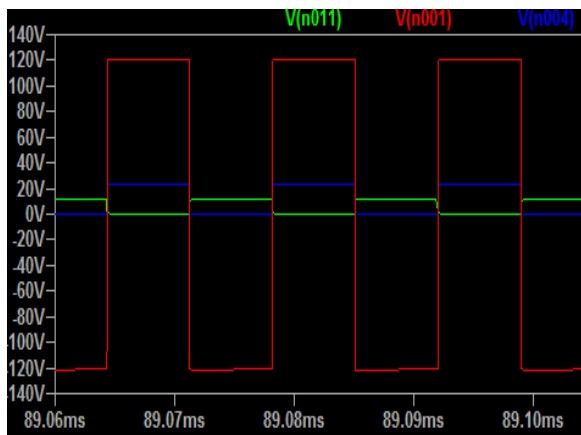


Fig.15. Waveshape of MOSFET gate drive signal and voltage waveshape across transformer winding.

Fig.15. shows the MOSFET gate drive switching waveform (Vn011 – green color), voltage waveform across the primary winding of transformer (Vn004 – blue color) and voltage waveform across the secondary winding of transformer (Vn001 – Red). The primary winding of transformer has induced 12V PWM waveform (Fig.14.) and the secondary winding has induced $\pm 120V$. A ultra fast diode has connected between the

terminal of secondary winding of transformer and DC link capacitor for rectifying the -120V. As a result, it has obtained expected output voltage +120V DC, that shows in Fig.13.

V. CONCLUSION

The research paper represents a design of a new controller for the off-grid solar home system, that incorporates PWM solar charging and a DC-DC converter (12V to 120V). Those research works enhance some features such as surge voltage protection which is applied 65.24KV as spike voltage; short circuit protection which is tested at output load terminal to flow the current is 6mA; overload protection which is tested at output load terminal to obtain output voltage 54V and current 2.1A across the 500Watt load . Reducing self-power consumption is 30.51mW that are introducing a push switch mechanism and a fixed frequency algorithm. The overall testing techniques are performed in accordance with the battery voltage under various load conditions, taking into consideration all parameters. The design has compacted as a new controller including common ground single stage to integrate the PWM Solar charging and DC-DC conversion unit. The suitable charging range is 10Wp up to 400Wp solar panels and the suitable load connected range is 1 Watt up to 350Watt to predicate upon this simulated wave-shape analysis. That is introducing the soft start mechanism at zero duty cycle. The fixed frequency current control mode is used as voltage mode with designing a flyback transformer. However, the analog circuits for controlling parts are the goal of this study. There is no need for shielding to protect against EMI noise. Besides that, the unexpected noisy signals that eliminate the main signals in the presence of a high-frequency transformer are ignored by the analog circuits.

APPENDIX-A

TABLE II
MEASUREMENT OF SELF-POWER CONSUMPTION

Portion	Voltage (V)	Current (μA)	Power (mW)
PWM Solar Charger	12.27	53.96	0.662
DC-DC converter controller	12.27	994.59	12.2
voltage comparator	12.27	1221	14.99
Push switch mechanism	12.27	216.057	2.65
Total self-power consumption			30.51

APPENDIX-B

SURGE VOLTAGE PROTECTION TEST:

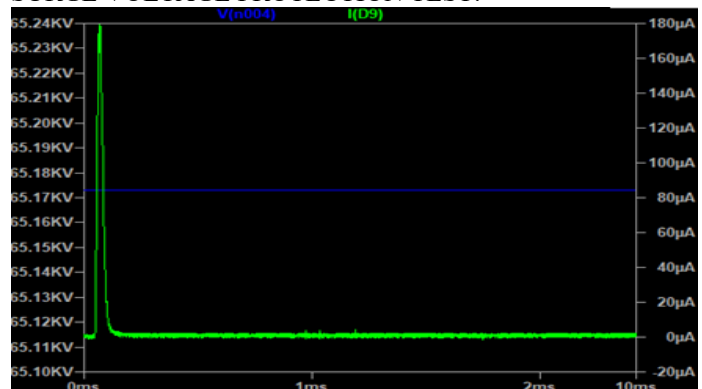


Fig 16: Voltage wave form across the solar panel during lightning voltage

APPENDIX-C

OVERLOAD PROTECTION TEST:

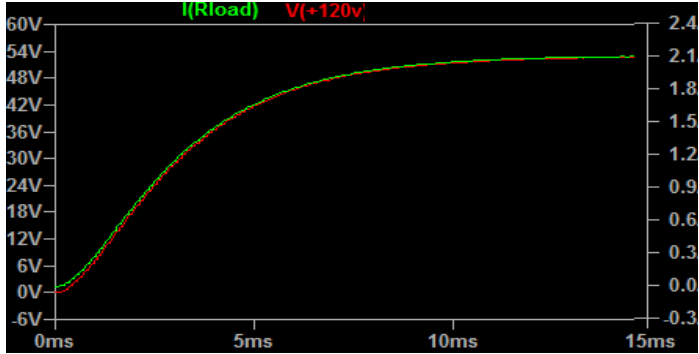


Fig 17: Voltage and current waveform under overload condition.

APPENDIX-D

SHORT CIRCUIT PROTECTION TEST:

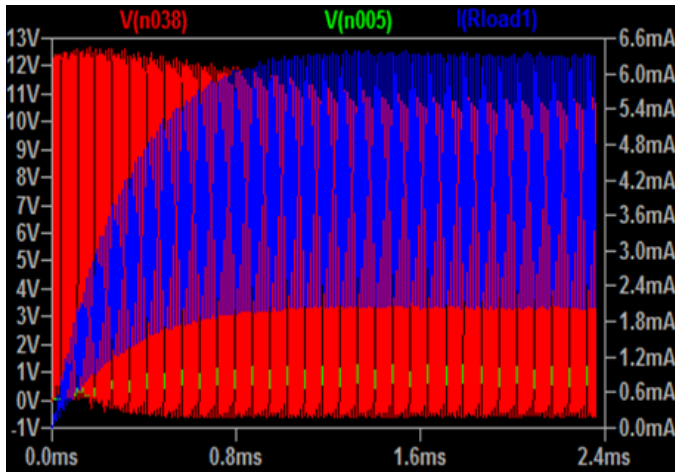


Fig 18: Voltage and current waveform under short circuit condition.

ACKNOWLEDGMENT

I would like to express my very great appreciation to the School of Electrical Engineering, Universiti Teknologi MARA (UiTM), Shah Alam, Selangor, Malaysia for knowledge and facilities.

REFERENCES

[1]. Aldrin Claytus Vaz, C Gurudas Nayak, and Dayananda Nayak, "Pulse Width Modulation based Solar Charge Controller", IEEE Xplore, Proceedings of the Third International Conference on Electronics Communication and Aerospace Technology [ICECA 2019] IEEE Conference Record # 45616, ISBN: 978-1-7281-0167-5, 2019.

[2]. Soha H. Metwally, Xiaolei Zhang, Sidra Ali, and Harish S. Krishnamoorthy, Senior Member, IEEE, "Solar PV and BESS based Home Energy System", 978-1-5386-9284-4/19, 2019.

[3]. Adel El-Shahat, Rami J. Haddad, Joseph Courson, Austin Martenson, Aaron Mosley, "Solar-Powered House System Design", IEEE, Auckland University of Technology. Downloaded on June 01, 2020; 978-1-7281-0137-8/19, 2019.

[4]. Kennedy Aganah, James Chukwuma, Mandoye Ndoye, "A Review of Off-Grid Plug-and-Play Solar Power Systems: Toward a New "I

Better Pass My Neighbor" Generator", 2019 IEEE PES/IAS Power Africa, 978-1-7281-1010-3/19.

[5]. Tahsina Hossain Loba, Khosru M. Salim, "Design and Implementation of a Micro-Inverter for Single PV Panel based Solar Home System", IEEE, 978-1-4799-0400-6/13, 2013.

[6]. Mofakkarul Islam, IEEE Member, Md. Abul Bashir Sarkar, "An Efficient Smart Solar Charge Controller for Standalone Energy Systems", IEEE, 2015 International Conference on Electrical Drives and Power Electronics (EDPE), 978-1-4673-7376-0/15, 2015.

[7]. Ivomir Antonov, Hristiyan Kanchev and Nikolay Hinov, "Study of PWM Solar Charge Controller Operation Modes in Autonomous DC System", IEEE, University of London. Downloaded on July 10, 2020 at 12:11:54 UTC from IEEE Xplore, 978-1-7281-4556-3/19, 2019.

[8]. Parag K. Atri, P. S. Modi and Nikhil Shashikant Gujar, "Comparison of Different MPPT Control Strategies for Solar Charge Controller", Auckland University of Technology. Downloaded on June 03, 2020 at 16:34:58 UTC from IEEE Xplore, 978-1-7281-6575-2/20, 2020.

[9]. Onur Ozdal MENGI, Ismail Hakkı ALTAS, "An Off-Grid PV/SC Green Energy Production System", 2015-IEEE.

[10]. M. Nassereddine, M. Nagrial, J. Rizk, A. Hellany, "Design of Low Cost and High Efficiency Smart PV Solar System for Sustainable Residential Home", IEEE International multidisciplinary Conference on engineering Technology, 978-1-5386-4500-0/18, 2018.

[11]. Chihchiang Hua and Chihming Shen, "Control of DC/DC Converters for Solar Energy System with Maximum Power Tracking", IEEE, Department of Electrical Engineering, National Yunlin University of Science & Technology, Taiwan., 2018.

[12]. Bhakti B. Baliwant, Ankita R. Gothane and V. B. Waghmare, "Hardware Implementation of DC-DC SEPIC Converter for Applications of Renewable Energy Using PWM Based Charge Controller", Proceedings of the Third International Conference on Electronics Communication and Aerospace Technology [ICECA 2019], IEEE Conference Record # 45616, IEEE Xplore ISBN: 978-1-7281-0167-5/19.

[13]. Taoufikul Islam, M. Abdul Awal, "Efficient Load and Charging Method for Solar Powered Home Lighting System of Bangladesh", IEEE, 2014.

[14]. Sravankumar Jogunuri, Ravish Kumar, Deepak Kumar, "Sizing an Off-Grid Photovoltaic System (A Case Study)", IEEE, International Conference on Energy, Communication, Data Analytics and Soft Computing (ICECDS-2017), 978-1-5386-1887-5/17, 2017.

[15]. Miss. Bhakti B. Baliwant, Miss. Ankita R. Gothane, Prof. V. B. Waghmare, "PWM Based Charge Controller for Renewable Energy Applications Using SEPIC Converter", Proceedings of the Third International Conference on Computing Methodologies and Communication (ICCMC 2019) IEEE Xplore Part Number: CFP19K25-ART. ISBN: 978-1-5386-7808-4, 2019.

[16]. Ubaid U. Khan, Musa Raheem, Suleman Ata, Z. H. Khan, "Design and Implementation of a Low-Cost MPPT Controller for Solar PV System", International Conference on Open Source Systems and Technologies (ICOSST), 978-1-5090-5586-9/16, 2016.

[17]. Alpesh M. Patel, Sunil Kumar Singal, "Off Grid Rural Electrification Using Integrated Renewable Energy System, IEEE, ", 978-1-4673-8962-4/16, 2016.

[18]. Alexandra POPESCU, Flaviu Mihai FRIGURA-ILIASA, "Computer Based Model for an Off-Grid Photovoltaic System with no DC – DC Adapter", IEEE 17th World Symposium on Applied Machine Intelligence and Informatics, January 24–26, Herl'any, Slovakia, 978-1-7281-0250-4/19, 2019.

[19]. Anusha Ramachandran, Sairam Mannar, Ashok Jhunjhunwala, "Inverterless Solar- DC System Design for OffGrid and Near Off-Grid Indian Homes", IEEE, 978-1-5090-3498-7/16, 2016.

[20]. Ashita Victor, Dharmendra Kumar Mahato, Amit Pundir, Geetika Jain Saxena, "Design, Simulation and Comparative Analysis of Different Types of Solar Charge Controllers for Optimized Efficiency", IEEE, ISBN: 978-1-7281-5204-2/19, 2019.

- [21]. Nupur Khara, Nancy Rana, Narendiran SI, Sarat Kumar Sahoo, Balamurugan M, S.Prabhakar Karthikeyan, I. Jacob Raglend, "Design of Charge Controller for Solar PV Systems", IEEE, International Conference on Control, Instrumentation, Communication and Computational Technologies (ICCICCT), 978-1-4673-9825-1/15, 2015.
- [22]. Ahana Malhotra, Dr.Prema Gaur, "Comparative Study of DC-DC Converters in Solar Energy Systems" IEEE, 978-1-4799-3080-7114, 2014.
- [23]. A.K. Podder, K. Ahmed, N. K. Roy and P.C. Biswas, "Design and Simulation of an Independent Solar Home System with Battery Backup", IEEE, Proceedings of the 2017 4th International Conference on Advances in Electrical Engineering (ICAEE), 28-30 September, Dhaka, Bangladesh, 978-1-5386-0869-2/17, 2017.
- [24]. Preethishri R.S and K. Kalai selvi, "The Photovoltaic Module fed Push Pull Converter with MPPT Controller for solar Energy Applications" 1st IEEE International Conference on Power Electronics, Intelligent control and Energy Systems (ICPEICES-2016), 978-1-4673-8587—9/16, 2016.
- [25]. Soumya Shubhra Nag, Suman Mandal, Santanu Mishra, "Solar PV Based DC Power Supply for Rural Homes with Analog, Multiplier-less MPPT Controller", IEEE, 987-1-5386-1127-2/17, 2017.
- [26]. Matthew Wells, "Model of Smart Solar PV Charge Controller", IEEE, 978-1-4244-9877-2/11, 2011.
- [27]. S. Y. Wong, A. Chai, "An Off-grid Solar System for Rural Village in Malaysia", IEEE, 978-1-4577-0547-2/12, 2012.
- [28]. Mingzhi Zhao, Zhizhang Liu, "Design and Application of Off-grid Solar PV System in Inner Mongolia of China", IEEE, International technology cooperation project from Ministry of Science and Technology of China, 978-1-4244-2487-0/09, 2009.
- [29]. ShaoWei Xie, FuBingJin, "Low Power Consumption Solar PV Charge Controller for Telemetry System", IEEE, 978-1-4673-9613-4/16, 2016.
- [30]. Nakago Yuki, Umeda Takashi, Ute Ryo, Fukui Masahiro, "Study of the DC-DC Converter Using SiC-MOSFET For Battery Charger", IEEE, 15th International Symposium on Communications and Information Technologies (ISCIT), 978-1-4673-6820-9/15, 2015.
- [31]. Mihir Pathare, Vimith Shetty, Diptarka Datta, Rajeev Valunekar, Aniket Sawant, Shreenivas Pai, "Designing and Implementation of Maximum PowerPoint Tracking (MPPT) Solar Charge Controller", IEEE, International Conference on Nascent Technologies in the Engineering Field (ICNTE-2017), 978-1-5090-2794-1/17, 2017.
- [32]. Apurva Jain, Deepu Vijay M, G. Bhuvanewari, Bhim Singh, "Design and Simulation of a Solar Powered DC Home with Grid and battery back-up", IEEE, 978-1-4673-8962-4/16, 2016.
- [33]. Julie Cynthia Rante, Alexander Patras, Lianly Rompis, "Design of a Solar Micro Power Plant for Home Lighting", IEEE, 978-1-5386-5721-8/18, 2018.
- [34]. Kapat, S. "Reconfigurable Periodic Bifrequency DPWM With Custom Harmonic Reduction in DC-DC Converters", IEEE Transactions on Power Electronics, 31(4). <https://doi.org/10.1109/TPEL.2015.2462111>, 2016.
- [35]. Su, J. P., Wang, Y. P., Tsai, M., & Chiu, R.. EMI Shielding Solutions for RF SiP Assembly. Proceedings of Technical Papers - International Microsystems, Packaging, Assembly, and Circuits Technology Conference, IMPACT, 2019-October. <https://doi.org/10.1109/IMPACT47228.9024991>
- [36]. Santanu Kapat, Member, IEEE, "Multi-Band Mixed-Signal Hysteresis Current Control for EMI Reduction in Switch-Mode Power Supplies" IEEE, 978-1-4673-9550-2/16, 2016.
- [37]. Marc Pous, Marco A. Azpúrua, Ferran Silva, "APD Outdoors Time-Domain Measurements for Impulsive Noise characterization", IEEE, Proc. of the 2017 International Symposium on Electromagnetic Compatibility - EMC EUROPE 2017, Angers, France, September 4-8, 978-1-5386-0689-6/17, 2017.
- [38]. Journal of Physics: Conference Series, 1500(1). <https://doi.org/10.1088/1742-6596/1500/1/012004>
- [39]. Abdelilah, B., Mouna, A., M'Sirdi, N. K., & Hossain, A. El. Solar charge controller with a data acquisition system based on arduino.

Lecture Notes in Electrical Engineering, 519, 412–420. https://doi.org/10.1007/978-981-13-1405-6_49, 2019.



Mohammad Shariful Islam received the Diploma in Engineering (Electronics Technology) from Comilla Polytechnic Institute, Comilla, Bangladesh, in 2003, Bachelor of Science in Electrical & Electronics Engineering (EEE) from United International University (UIU), Dhaka, Bangladesh in 2010

and he is currently pursuing the Master of Science in Electrical Engineering (Research) at Universiti Teknologi MARA (UiTM), Selangor, Malaysia.

From Sep 2003 until Aug 2010, he had been an engineer at various companies. In Sep 2010, he had been a Manager in R&D Department, Solar Intercontinental (SOLAR-IC) Ltd, until May 2017. He is the author of one book, more than 7 articles, and more than 30 designed for solar home system and home appliances. His research interests include solar energy management, renewable energy sources, analogue circuit, solar nano-grid, solar micro-grid, Net-Zero-Energy (NZE) house, battery charging mechanism, electrical vehicle DC-DC converter, energy efficient mechanism, holistic design optimization of power electronics converters and power electronics engineering.



Hasmaini Mohamad received the B. Eng, M.Eng and Ph.D degrees from the University of Malaya in 1999, 2004 and 2013 respectively. She started her career as a lecturer in Universiti Teknologi MARA in 2003 where currently she is an Associate Professor at the Centre for Electrical Power Engineering studies, Faculty of Electrical

Engineering. Apart from that, she has published more than 50 journal papers including high impact ISI journals and 20 conference papers. Her major research interest includes islanding operation of distributed generation, hydro generation, load sharing technique, and load shedding scheme.



Siti Zaliha Mohammad Noor obtained Bachelor of Electrical Engineering (Hons) in 2005, M Sc Power Electronics in 2008 and Ph.D in Electrical Engineering in 2018 from Universiti Teknologi MARA (UiTM), Malaysia. She is currently a Senior Lecturer at the School of Electrical Engineering, UiTM. She has authored and co-authored over 40 technical papers

in indexed international journal and conferences. Her research interests are renewable energy, power electronics, modeling

and simulation, signal processing and embedded controller applications. She is a Certified Energy Manager, Certified Professional in Measurement and Verification (CPMV), and Qualified Person (QP) SEDA Malaysia Grid-Connected Solar Photovoltaic Systems Design. She is also attached to industry collaborations as the Subject Matter Expert (SME) for the Photovoltaic (PV) system and energy audit.